INTERNATIONAL JOURNAL FOR NUMERICAL METHODS IN FLUIDS, VOL. 14, 1135–1149 (1992)

NUMERICAL SIMULATION OF FULLY NON-LINEAR STEADY FREE SURFACE FLOW

F. LALLI, E. CAMPANA AND U. BULGARELLI

INSEAN, Italian Ship Model Basin, Via di Vallerano 139, I-00128 Rome, Italy

SUMMARY

The fully non-linear free surface potential flow past a 2D non-lifting body is computed. The numerical method is based on the simple layer integral formulation; the non-linear solution is obtained by means of an iterative procedure. Under some hypotheses, viscosity effects at the free surface are considered. All the numerical results obtained have been tested against analytical solutions and experimental results.

KEY WORDS Free surface flow Non-linear effects Free surface boundary layer BEM

1. MATHEMATICAL FORMULATION

We consider the mathematical formulation governing the two-dimensional steady state potential flow due to the motion of a non-lifting body $\mathscr{B}$ submerged in a fluid of infinite depth. The extension to three-dimensional cases can be easily obtained. The fluid domain $\mathscr{D}$ is bounded on the upper part by a free boundary $\mathscr{S}$ and unbounded in the other directions. The frame of reference is assumed to be fixed with the body: the x-axis is oriented as the uniform stream $\mathbf{U}=(U, 0)$, the y-axis is positive upwards and the Cartesian equation of the undisturbed free surface is given by $y=0$ (see Figure 1). We assume that the fluid velocity $\mathbf{u}=(u, v)$ can be written as

$$\mathbf{u}=\nabla\phi,$$

where

$$\phi(x, y)=Ux+\varphi(x, y). \tag{1}$$

In (1) the term Ux is the free stream potential and the term $\varphi(x, y)$ takes into account the interaction between the free surface and the body. The potential $\phi(x, y)$ satisfies Laplace equation inside $\mathscr{D}-\bar{\mathscr{B}}$:

$$\nabla^2\phi(x, y)=0, \quad (x, y)\in\mathbb{R}^2-\bar{\mathscr{B}}\cap\{y:-\infty<y\leqslant\eta(x)\}, \tag{2}$$

where $\bar{\mathscr{B}}=\mathscr{B}\cup\partial\mathscr{B}\subset\mathbb{R}^2$ is the body and $y=\eta(x)$ is the Cartesian equation of the free boundary $\mathscr{S}$.

The boundary condition on the body surface is

$$\phi_n(x, y)=0 \quad \text{on } \partial\mathscr{B}. \tag{3}$$

Furthermore, two conditions are necessary at the free surface $\mathscr{S}$. The kinematic one follows from the property of an interface, which cannot be crossed by the fluid: the normal velocities of the fluid

0271–2091/92/101135–15$07.50

Received February 1991
Revised August 1991

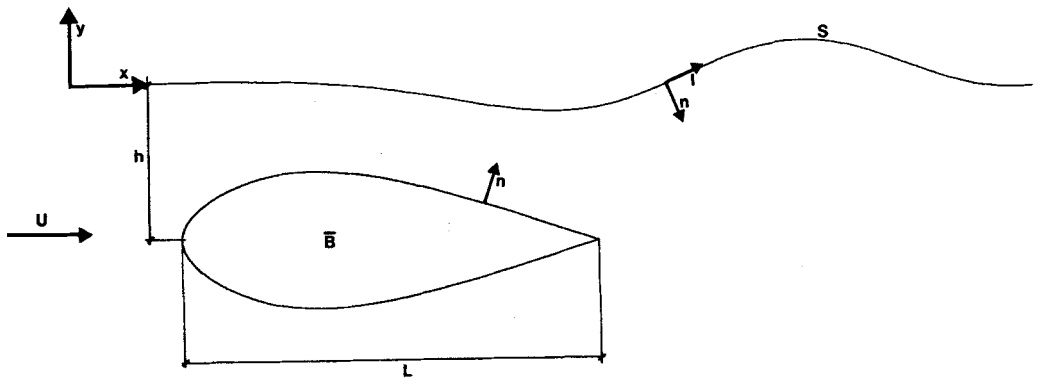

Figure 1. Definition sketch of the problem

and of the interface itself must be equal. In particular, for the steady state case they must be equal to zero:

$$\phi_x(x, y)\eta_x(x)-\phi_y(x, y)=0 \quad \text{on } \mathscr{S}. \tag{4}$$

The dynamical boundary condition follows from the assumption that the pressure over the free surface is constant. The Bernoulli equation, in which we have assumed that surface tension effects are negligible, gives

$$\eta(x)=\frac{1}{2g}[U^2-\nabla\phi(x, y)\cdot\nabla\phi(x, y)] \quad \text{on } \mathscr{S}. \tag{5}$$

Finally, a condition at infinity must be imposed:

$$\lim_{x\to-\infty} |\nabla\phi|=U. \tag{6}$$

The exact formulation of free surface potential flows is characterized by the presence of a double non-linearity, since conditions (4) and (5), both containing quadratic terms, have to be applied on a curve whose shape is itself an unknown of the problem.

For computational purposes we need to obtain a unique boundary condition for $\mathscr{S}$ by eliminating $\eta(x)$ between (4) and (5). Differentiating (5) with respect to x (remembering that the RHS is evaluated at $y=\eta(x)$) and upon substitution in (4), the following unified condition is finally obtained:

$$\phi_x(x, \eta)\nabla\phi(x, \eta)\cdot\nabla\phi_x(x, \eta)+\phi_y(x, \eta)[\nabla\phi(x, \eta)\cdot\nabla\phi_y(x, \eta)+g]=0. \tag{7}$$

In obtaining the former condition, we must require that

$$\nabla\phi(x, \eta)\cdot\nabla\phi_y(x, \eta)\neq -g. \tag{8}$$

Thus the vertical component of the fluid acceleration must be different from $-g$; this limit concerns the flow stability (with respect to the wave-breaking phenomenon).

The problem described so far can be revisited by considering a curvilinear abscissa l defined along the free boundary, which in the steady state case is a streamline of the flow. Therefore the set

of boundary conditions (4), (5), (7) can be rewritten as

$$\phi_l(x, \eta)\eta_l(x)=\phi_y(x, \eta), \tag{9}$$

$$\eta(x)=\frac{1}{2g}[U^2-\phi_l^2(x, \eta)], \tag{10}$$

$$\phi_l^2(x, \eta)\phi_{ll}(x, \eta)+g\phi_y(x, \eta)=0. \tag{11}$$

It is worth noticing that (9)–(11) are formally identical for 2D and 3D cases; this formulation seems to be the most natural for the interface conditions, especially in view of dealing numerically with the fully non-linear problem in both two and three dimensions. The equivalence between (4), (5) and (9), (10) is obvious, while for (7) and (11) it can be easily shown that

$$\phi_l^2\phi_{ll}=\nabla\phi\cdot\nabla\phi\frac{\partial(\nabla\phi\cdot\mathbf{l})}{\partial l}=\nabla\phi\cdot\nabla\phi\left(\frac{\partial\nabla\phi}{\partial l}\cdot\mathbf{l}+\nabla\phi\cdot\frac{\partial\mathbf{l}}{\partial l}\right),$$

with $\mathbf{l}=(\alpha, \beta)$ the unit vector tangent to the free boundary (see Figure 1); but, if $K=\eta_{xx}/(1+\eta_x^2)^{3/2}$ is the curvature and $\mathbf{n}=(\beta, -\alpha)$ is the internal normal unit vector,

$$\nabla\phi\cdot\frac{\partial\mathbf{l}}{\partial l}=-K\nabla\phi\cdot\mathbf{n}=0$$

and

$$\begin{aligned}\nabla\phi\cdot\nabla\phi[\nabla(\nabla\phi)\cdot\mathbf{l}]\cdot\mathbf{l}&=(\phi_x^2+\phi_y^2)(\alpha^2\phi_{xx}+2\alpha\beta\phi_{xy}+\beta^2\phi_{yy})\\&=\phi_x^2\phi_{xx}+2\phi_x\phi_y\phi_{xy}+\phi_y^2\phi_{yy},\end{aligned}$$

since, of course, $\alpha\phi_y=\beta\phi_x$.

In the next section we will discuss the numerical solution of the problem (1)–(3), (6), (10), (11) and its linearized versions.

2. LINEARIZED FORMULATIONS: SOME DISCUSSIONS ABOUT NUMERICAL IMPLEMENTATION

The mathematical model outlined before describes the wave resistance problem, one of the typical topics in naval hydrodynamics.

In this work the fully non-linear free surface flow will be computed by means of a numerical scheme implying an iterative procedure: the first step will be the solution of the linearized problem.

The simplest linear formulation is obtained by assuming the flow to be a small perturbation of the uniform stream; the shape of the free surface must, of course, be very smooth. Making use of (1) and neglecting the non-linear terms in both (4) and (5), we get the linearized interface conditions

$$U\eta_x=\varphi_y \qquad \text{on } y=0 \tag{12}$$

$$\eta=-\frac{U}{g}\varphi_x \qquad \text{on } y=0 \tag{13}$$

and the well known Neumann–Kelvin condition

$$\varphi_{xx}+\frac{g}{U^2}\varphi_y=0 \quad \text{on } y=0. \tag{14}$$

It is worth noticing that, for this formulation, theorems for solution existence and uniqueness have been given in Reference 1. This kind of linearization can give reasonable results not only when the body velocity is small enough but also if the body is either very slender or deeply submerged. Dawson[2] proposed another type of linearized formulation which seems to be more realistic for bodies moving near the free surface and for floating bodies. As basis fluid motion he assumed the free surface flow past the body with zero Froude number (the free surface behaves like a rigid plane wall). Following Dawson, we write

$$\phi(x, y)=\varphi_0(x, y)+\varphi_1(x, y), \tag{1'}$$

where φ_0 is the just defined basis flow, characterized by the property $\varphi_{0y}(x, 0)=0$, and φ_1 is the free surface potential. Neglecting the squares of this last term as well as its products with η, we get Dawson's linear formulation

$$\varphi_{0x}\eta_x=\varphi_{1y} \quad \text{on } y=0, \tag{12'}$$

$$\eta=\frac{1}{2g}[U^2-(\varphi_{0x}^2+2\varphi_{0x}\varphi_{1x})] \quad \text{on } y=0, \tag{13'}$$

$$\varphi_{0x}^2\varphi_{1xx}+2\varphi_{0x}\varphi_{0xx}\varphi_{1x}+g\varphi_{1y}=-\varphi_{0x}^2\varphi_{0xx} \quad \text{on } y=0. \tag{14'}$$

Dawson also proposed a very simple and effective numerical procedure based on the simple layer potential formulation; perhaps the Dawson method could be considered as the natural extension to naval hydrodynamics of the method of Hess and Smith.[3] The conventional naval hydrodynamics approach implies the use of a very complicated Green function[4] satisfying the linear free surface conditions. Two important advantages are therefore connected with Dawson idea: first, the simple layer potential is very easy to treat computationally and the distribution of panels on the free surface allows one to consider different boundary conditions; secondly, extension to the non-linear case is also possible without introducing any substantial variation in the procedure, which can maintain the original simplicity also for the non-linear problem. A peculiarity of the Dawson scheme is the approximation proposed for the derivative $\partial\varphi_{1x}/\partial x$ in the convective term of (14'), i.e. a second-order four-point upwind operator (see below) characterized by a very light numerical damping. His method has become quite popular for its simplicity and effectiveness; in the wake of Dawson, several numerical papers have appeared in the literature. Some authors deal with the linear problem, discussing the consistency of the different kinds of linearization[5] proposed in the literature, others deal with enforcement of the radiation condition,[6, 7] while in Reference 8 general criteria are suggested for studying the numerical properties (stability, numerical damping and dispersion) of discrete schemes.

Many authors have pointed out the limitations of the linear formulation: starting from the Dawson solution, the subsequent aim is suggested to be the solution of the non-linear problem. References 9–12 deal with the second-order problem obtained by means of Taylor expansion. At the same time some researchers have started to work on the fully non-linear problem. In References 13 and 14 moving panel methods are proposed in which the exact non-linear conditions are applied at the free surface, computed step by step, but the features of the numerical method were not stressed and no convergence problem was mentioned. Nevertheless, severe difficulties will appear as soon as any attempt to update the linear solution iteratively is made; these difficulties grow, of course, with increasing Froude number.

In the present work, with the aid of a two-dimensional test case, it will be shown how the range of applicability of moving panel methods depends on the particular numerical scheme adopted: we propose an algorithm which enlarges this range.[15] Moreover, to further improve the model,

we develop a new dynamic boundary condition in which, under some hypotheses, the effects of viscosity at the free surface are taken into account.[15]

3. EFFECTS OF VISCOSITY AT THE FREE SURFACE

Typical gravity waves are lightly damped by the action of a superficial boundary layer. In fact, among the free surface phenomena, the presence of a thin boundary layer can also be considered. Although a rigid boundary is the commonest source of vorticity, in the case of a free boundary the vanishing of the tangential stresses generates vorticity and consequently a viscous boundary layer. All real fluid motions are of course rotational; although a flow can be nearly irrotational, the relatively small amount of vorticity present in thin layers can be crucial in determining the main flow characteristics, as in the case of lifting bodies.

In our analysis we start from the consideration that the irrotational motion does not fulfil the condition of zero tangential stresses at the free surface in the case of a free boundary with non-zero curvature. Consequently, we introduce in our model a partition of the flow field into an inviscid region, free from vorticity, and a thin viscous layer near the free boundary. Across this layer a vorticity jump, connected with the free surface curvature, is considered.

We do not study the flow details inside the boundary layer but take into account its effect on the external flow. Such an effect, however slight it may be (see Figure 4), does improve the numerical behaviour of the iterative scheme, allowing the non-linear model to work for higher Froude numbers without introducing any artificial numerical recipe.

To evaluate the viscous effects, we start from the steady Navier–Stokes equation written for $y=\eta(x)$:

$$\nabla(\tfrac{1}{2}\,\mathbf{u}\cdot\mathbf{u}+g\eta)=\mathbf{u}\times\boldsymbol{\omega}\;-\nu\nabla\times\boldsymbol{\omega}\quad\text{on }\mathscr{S}, \tag{15}$$

where $\boldsymbol{\omega}=(0,0,\omega)$ is the fluid vorticity and assuming zero atmospheric pressure.

Since the integral of the LHS of (15) is path-independent, we can integrate both sides along $\mathscr{S}$, which in the steady flow is a streamline. Requiring that

$$\lim_{x\to-\infty}|\mathbf{u}|=U,$$

we obtain

$$\eta=\frac{U^2}{2g}-\frac{1}{2g}\,\mathbf{u}\cdot\mathbf{u}-\frac{\nu}{g}\int_{-\infty}^{l}\nabla\times\boldsymbol{\omega}\cdot\mathbf{l}\,\mathrm{d}l'\quad\text{on }\mathscr{S}, \tag{16}$$

since $\mathbf{u}\times\boldsymbol{\omega}\cdot\mathbf{l}=0$.

The kernel of the curvilinear integral can be transformed as

$$\nabla\times\boldsymbol{\omega}\cdot\mathbf{l}\,\mathrm{d}l'=-\frac{\partial\omega}{\partial n}\,\mathrm{d}l', \tag{17}$$

where the normal unit vector n is oriented inwards. By substituting (17) into (16), we get

$$\eta=\frac{U^2}{2g}-\frac{1}{2g}\,\mathbf{u}\cdot\mathbf{u}+\frac{\nu}{g}\int_{-\infty}^{l}\frac{\partial\omega}{\partial n}\,\mathrm{d}l'\quad\text{on }\mathscr{S}. \tag{18}$$

The normal derivative of ω, if the viscous layer is sufficiently thin, can be expressed as the ratio between the vorticity jump across the boundary layer and its thickness δ:

$$\frac{\partial\omega}{\partial n}\simeq-\frac{\Delta\omega}{\delta}. \tag{19}$$

The expression of $\Delta\omega$ can be evaluated as[16]

$$\Delta\omega = 2K|\nabla\phi|, \tag{20}$$

where K is the free boundary curvature defined previously. Moreover, an estimation of the boundary layer thickness can be given by[16]

$$\delta \simeq \sqrt{\left(\frac{Uv}{g}\right)}. \tag{21}$$

Furthermore, we observe that the velocity distribution in the fluid domain can be decomposed as

$$\mathbf{u} = \nabla\phi + \mathbf{u}_v,$$

where $\mathbf{u}_v$ is required to satisfy

$$\nabla \cdot \mathbf{u}_v = 0, \qquad \nabla \times \mathbf{u}_v = \omega.$$

In particular, the velocity at the free boundary can be thought as the sum of $|\nabla\phi|$ and the jump $\Delta|\mathbf{u}_v|$ of the rotational component across the boundary layer. This jump can be estimated as[16]

$$\Delta|\mathbf{u}_v| \simeq \delta\Delta\omega.$$

Hence we have

$$|\mathbf{u}| = |\nabla\phi| + \Delta|\mathbf{u}_v| \simeq |\nabla\phi| + \delta\Delta\omega = |\nabla\phi| + 2K\delta|\nabla\phi|. \tag{22}$$

By introducing (19)–(22) in (18), neglecting terms of order δ^2, we get

$$\eta(x) = \frac{1}{2g}\{U^2 - [1+\lambda(x)]\phi_l^2(x,\eta)\} + \Lambda(x,\eta), \tag{23}$$

where

$$\lambda = 4\delta K, \qquad \Lambda = -2\frac{v}{g\delta}\int_{-\infty}^{l} K\phi_{l'}\,\mathrm{d}l'.$$

The unified free surface boundary condition is obtained from (9) and (23) as

$$[1+\lambda(x)]\phi_l^2(x,\eta)\phi_{ll}(x,\eta) + g\phi_y(x,\eta) = \mu(x,\eta)\phi_l^2(x,\eta), \tag{24}$$

where

$$\mu = 2\left(\delta K_l\phi_l + \frac{v}{\delta}K\right).$$

We observe that in the limiting case of $\delta \to 0$ the terms λ, Λ and μ vanish and the inviscid conditions (10) and (11) can be obtained respectively from (23) and (24).

4. THE DISCRETE MODEL

The numerical solution of the mathematical model given in Section 1 is computed by means of a simple layer formulation.[3] Bearing in mind the expression (1) for the potential ϕ, we write

$$\varphi(x,y) = \int_{\partial\mathscr{B}} \sigma(\xi_1,\xi_2)\log r\,\mathrm{d}\Sigma + \int_{\mathscr{S}} \sigma(\xi_1,\xi_2)\log r\,\mathrm{d}\Sigma, \tag{25}$$

where

$$r=\sqrt{[(x-\xi_1)^2+(y-\xi_2)^2]}$$

and $\sigma(\xi_1, \xi_2)$ is the unknown simple layer potential density.

To describe the discretization technique, we consider now the 2D linear problem of the free surface flow past a submerged circular cylinder; for this case analytical solutions are available.[17] The velocity potential $\phi(x, y)$ is experessed as

$$\phi(x, y)=Ux+Ua^2\left(\frac{x}{x^2+(y+h)^2}+\frac{x}{x^2+(y-h)^2}\right)+\int_{-\infty}^{\infty}\sigma(\xi_1)\log\sqrt{[(x-\xi_1)^2+y^2]}\,\mathrm{d}\xi_1, \quad (26)$$

with a and h respectively the radius and depth of the circular cylinder; for the linear case the method of images is used. It must be noted that this formulation contains an approximation connected with the hypothesis of high submergence: using the dipole potential, the boundary condition on the cylinder is approximately satisfied, since the free surface potential contribution on the body surface cannot be corrected by a suitable dissymmetrical simple layer distribution. Anyway, this formulation has been used for the comparison with the analytical results proposed by Havelock.[17] Thus the Neumann–Kelvin condition (14), where the variables have been non-dimensionalized with respect to U and the diameter $2a$, can be developed as

$$\frac{\mathrm{d}^2}{\mathrm{d}x^2}\int_{-\infty}^{\infty}\sigma(\xi_1)\log|x-\xi_1|\,\mathrm{d}\xi_1-\frac{\pi}{Fr^2}\sigma(x)=-\frac{x(x^2-3h^2)}{(x^2+h^2)^3}, \quad (27)$$

where the Froude number is defined as $U/\sqrt{(2ag)}$. This is an integral equation of the second type; in order to obtain the numerical solution, we discretize a finite part of the undisturbed free surface (where the simple layer potential is defined) by means of the collocation method. For the unknown function $\sigma(x)$ a piecewise constant variation is assumed:

$$\sum_{k=1}^{N}\sigma_k\left(\frac{\mathrm{d}}{\mathrm{d}x}I_k(x)\right)_{x=x_i}-\frac{\pi}{Fr^2}\sigma(x_i)=-\frac{x_i(x_i^2-3h^2)}{(x_i^2+h^2)^3}, \qquad i=1, \ldots, N, \quad (27')$$

where, denoting by L_k the generic linear boundary element of the free boundary,

$$I_k(x)=\frac{\mathrm{d}}{\mathrm{d}x}\int_{L_k}\log|x-\xi_1|\,\mathrm{d}\xi_1.$$

The derivative $\mathrm{d}/\mathrm{d}x$ which appears in (27′) has been implemented by a second-order finite difference scheme:[2]

$$\left.\frac{\delta f}{\delta x}\right|_i=\frac{10f_i-15f_{i-1}+6f_{i-2}-f_{i-3}}{6\Delta x}.$$

An operator of the upwind type has been chosen to enforce the radiation condition (6); in this case no boundary conditions are required at the furthest upstream nodes. The numerical behaviour of this scheme has been discussed in Reference 8, where it has been shown that the numerical damping and dispersion are respectively of fifth and first order. The scheme converges linearly, i.e. is of first order.

The term $I_k(x)$ can also be derived analytically:[7] in this case the radiation condition (6) must be imposed explicitly. Numerical experiments performed in this linear case have shown that the following conditions must be satisfied at the first node upstream to avoid numerical oscillations of the free surface before the body:

$$\varphi_{xx}(x_1, 0)=0, \qquad \varphi_y(x_1, 0)=0, \quad (28)$$

instead of the more obvious

$$\varphi_x(x_1, 0)=0, \qquad \varphi_y(x_1, 0)=0. \tag{29}$$

Of course, for the linear system closure no conditions must be required at the last node downstream. The validity of this choice is clearly observed in Figure 2(a). The free surface profile given by

$$\eta_i=-2Fr^2\frac{(h^2-x_i^2)}{(x_i^2+h^2)^2}-Fr^2\sum_{k=1}^{N}\sigma_k I_k(x_i), \qquad i=1, \ldots, N, \tag{30}$$

is plotted in Figures 2(b) and 2(c) in comparison with the analytical solution given in Reference 17. In Figure 2(b) the numerical solution obtained by means of finite difference implementation is plotted, while Figure 2(c) refers to the method employing analytical derivation of the term $I_k(x)$. In Figure 2(b) the numerical properties of the scheme demonstrated in Reference 8 can be observed: the wave amplitude is retained with good accuracy but for the wavelength the behaviour is not so good. Such behaviour can be improved with the second method described above, as shown in Figure 2(c).

Anyway, in the present work the full non-linear formulation has been implemented by means of the finite difference scheme, for its simplicity, since the main goal of this paper is to outline the features of the non-linear procedure. In a future work we will extend the method to the 3D case, implementing the more accurate scheme for $I_k(x)$.

Let us consider now the fully non-linear problem; we will refer, for simplicity, to the inviscid formulation (10) and (11) non-dimensionalized with respect to the body length L and the velocity U. The extension to the analogous conditions (23) and (24) is obvious, taking into account that all the terms including viscosity effects have been considered explicitly.

The body surface $\partial\mathscr{B}$ and part of the free surface $\mathscr{S}$, which is an unknown of the problem, are discretized by means of linear elements; as in the linear case, the simple layer density σ is assumed to be constant on every boundary element. During the iterative procedure the free boundary $\mathscr{S}$ is 'followed', step by step, by updating its discretization and, of course, the influence matrices. At the first step, to initialize the procedure, the potential flow and the shape of $\mathscr{S}$ are computed with the linear Dawson[2] formulation (12')–(14')

The iterative scheme consists of two cycles: an 'internal one, in which the non-linear system given by the boundary conditions (3) on $\partial\mathscr{B}$ and (11) on $\mathscr{S}$ is solved iteratively; when the solution of this system satisfies the required accuracy, the 'external' cycle updates the free surface configuration by using (10). Therefore at each external step (m) a complete internal cycle is performed. The (j)th step of the internal iterative procedure consists of solving the non-linear system

$$^{(j)}\phi_{n_i}=0 \quad \text{on } \partial\mathscr{B}, \tag{3'}$$

$$^{(j-1)}\phi_{l_i}^2\left(^{(m)}\alpha_i\frac{\delta}{\delta l}{}^{(j)}\varphi_{x_i}+{}^{(m)}\beta_i\frac{\delta}{\delta l}{}^{(j)}\varphi_{y_i}\right)+\frac{^{(j)}\varphi_{y_i}}{Fr^2}=0, \tag{11'}$$

in which the Froude number is defined with respect to the body chord. The quadratic term is considered explicitly with the values assumed at the previous step ($j-1$); condition (11') is imposed on the free surface updated at the previous external step (m). An underrelaxation is used: the value of the parameter must decrease as the Froude number grows. The finite difference operator $\delta/\delta l$ has been chosen with identical features to those described before for the operator $\delta/\delta x$ which compares in the linear case.

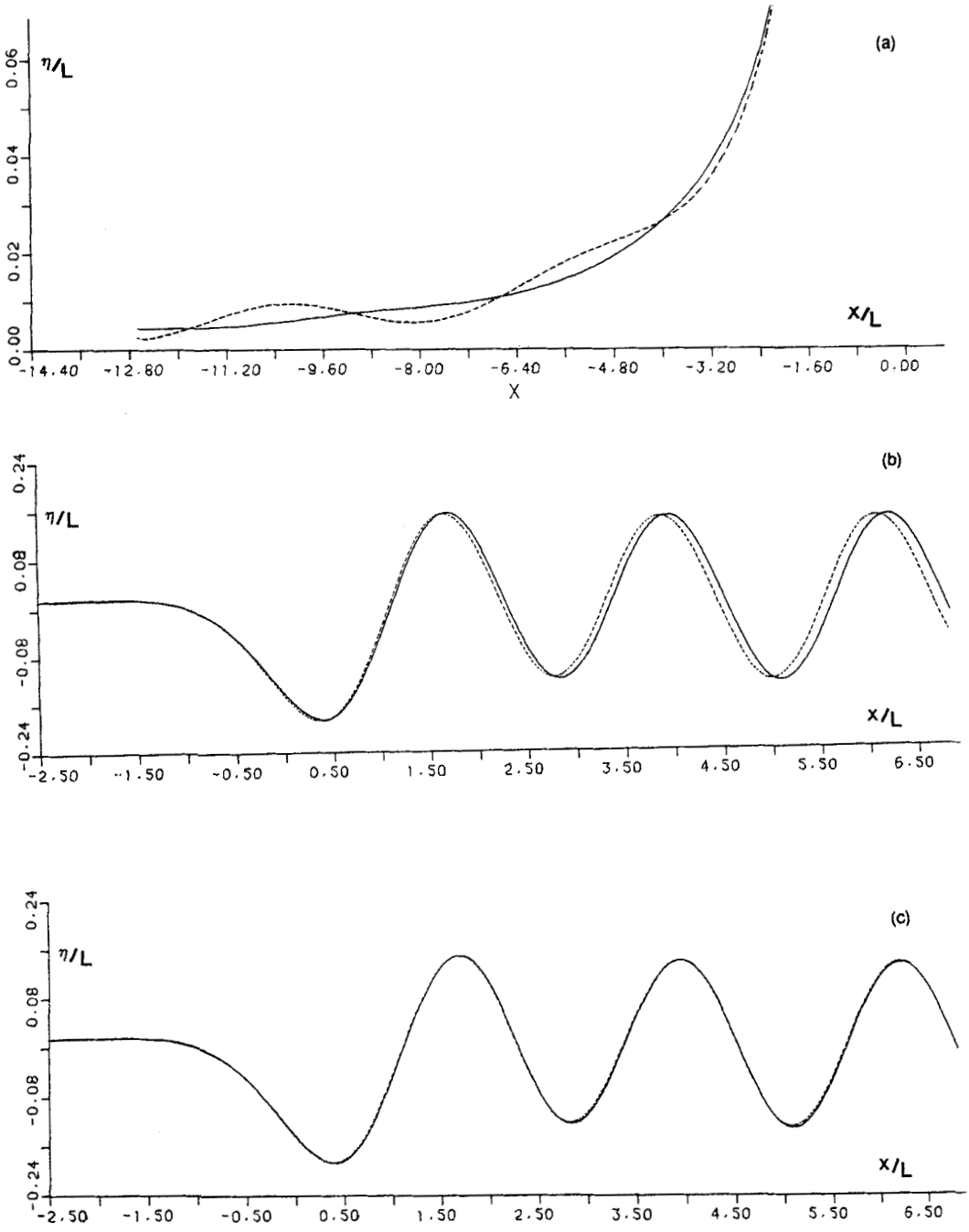

Figure 2. 2D surface waves due to a submerged dipole ($Fr=0{\cdot}6$, $h/L=1{\cdot}5$). The numerical results are obtained with 60 panels per wavelength. (a) Upstream part of the free surface obtained with the analytical derivative scheme[7] and with two different radiation conditions at the first node: ——, by imposing (28); – – –, by imposing (29). (b) Finite differences scheme[2] (– – –) and analytical solution[17] (——). (c) Analytical derivative scheme (– – –) and analytical solution (——)

The internal cycle is carried out until

$$\max|1-({}^{(j-1)}\phi/{}^{(j)}\phi)_i|<{}^{(m)}\varepsilon_{int},$$

where the tolerance ε_{int} has been chosen as a function of the external cycle current error in order to optimize the procedure.

Once the solution of the non-linear problem (3'), (11') is obtained, the wave elevation $\eta(x)$ is computed by means of the discretized form of (10):

$${}^{(m+1)}\eta_i=\frac{Fr^2}{2}(1-\phi_{l_i}^2). \tag{10'}$$

An underrelaxation parameter is used also for the external cycle, which is considered over when

$$\max|1-({}^{(m-1)}\eta/{}^{(m)}\eta)_i|<\varepsilon_{ext}.$$

Finally, when the convergence on the external cycle is reached, the wave resistance is computed by means of the Bernoulli equation

$$R_w=-\tfrac{1}{2}\sum_{i=1}^{N}(1-\phi_{l_i}^2)\mathbf{n}_i\cdot\mathbf{x}\,d_i \quad \text{on } \partial\mathscr{B},$$

where d_i is the (i)th boundary element length.

5. DISCUSSION OF NUMERICAL RESULTS

The aim of the present paper is to describe a numerical method whose main applications are in naval hydrodynamics for ship hull design purposes. Thus the determination of the wave-making

Table I

X	Y
0·00000	0·00000
0·00026	0·00623
0·00396	0·02465
0·01823	0·05379
0·04993	0·08975
0·10032	0·12624
0·16264	0·15710
0·22964	0·17806
0·30273	0·18655
0·37981	0·18517
0·45869	0·17520
0·53770	0·15813
0·61455	0·13649
0·68779	0·11309
0·75604	0·09035
0·81325	0·06980
0·86615	0·05003
0·91924	0·03017
0·96298	0·01383
0·99064	0·00350
1·00000	0·00000

drag is very important and we obtain it by means of pressure computation on the surface of the non-lifting body. Figure 1 shows the test case hydrofoil[18] used for the computations performed in this work; the shape of the hydrofoil is given in Table I. In Figure 3(a) is plotted the drag encountered by the body advancing in an unbounded fluid versus the number of body boundary elements (NPB) used, for different stretching techniques that concentrate the nodes near the leading and trailing edges. Such a drag must obviously be equal to zero (D'Alembert paradox), but unfortunately we see that the accuracy is not so good (all the computations have been

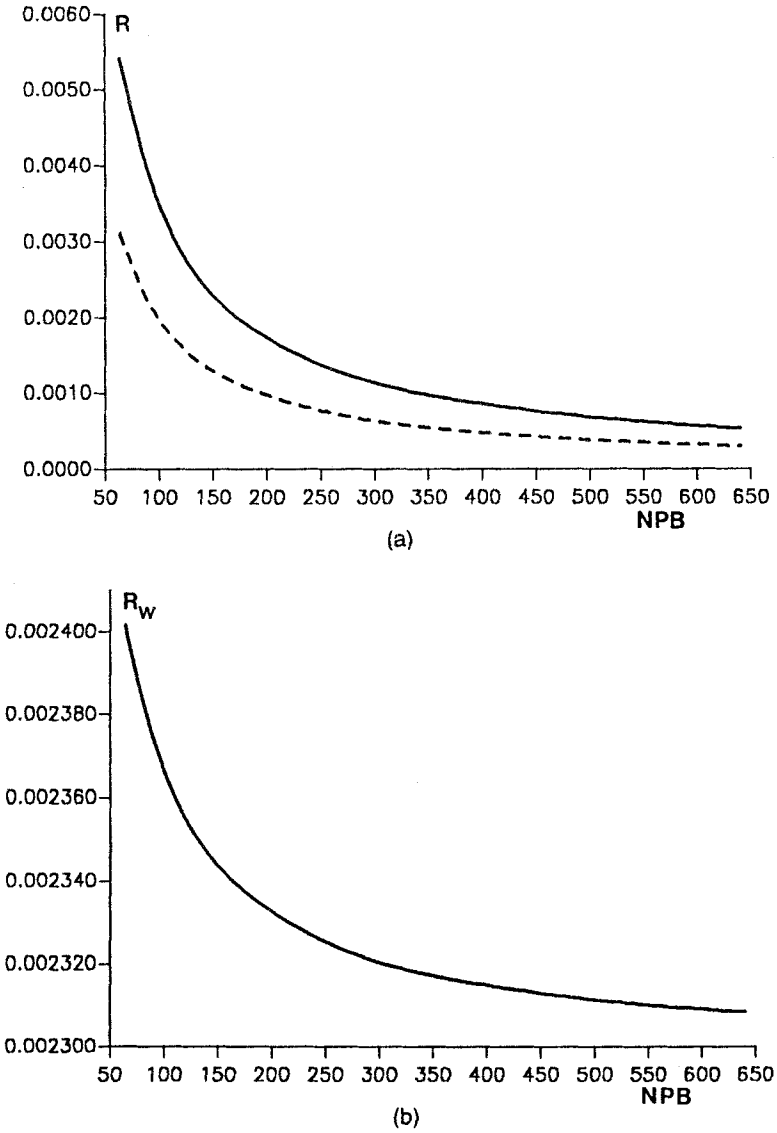

Figure 3. (a) Computed drag in the case of unbounded fluid. The nodes are distributed along the body surface according to a cosine (– – –) and a hyperbolic tangent (——) stretching. (b) Linear wave resistance versus number of elements on the body surface (NPB)

performed in double precision). It can be observed that if the computed potential flow does not fulfil the D'Alambert paradox with reasonable accuracy, the compatibility condition

$$\int_{\partial\mathscr{B}} \sigma \mathrm{d}\Sigma = 0$$

is also roughly verified.

In Figure 3(b) is plotted the linear wave resistance minus the drag computed in the absence of the free surface effects ($Fr = 0{\cdot}55$, $h/L = 1{\cdot}146\,78$) versus the number of body panels (250 panels are arranged on the free surface, with 30 elements per wavelength). For our computations we have therefore decided to arrange 256 panels on the body using a cosine-type stretching. On the free surface, making use of the strategy outlined in Reference 10, 700 panels have been used, with 60 elements per wavelength; one-third of the discretized free surface lies upstream with respect to the leading edge of the body.

The simplest non-linear algorithm used (the one proposed in References 13 and 14) consists of solving the system (3′), (11′) without requiring any accuracy every step, but updating $\mathscr{S}$ immediately by means of (10′); in other words, without the internal cycle of iterations described before. Considering the case of hydrofoil submergence $h/L = 1{\cdot}146\,78$, with this method no results can be computed for $Fr > 0{\cdot}47$ since the current error on the wave elevation grows indefinitely. In order to increase the Froude number range of applicability, the double-cycle scheme can be introduced; the range grows until $Fr = 0{\cdot}59$.

Moreover, the introduction of conditions (23) and (24), including viscous correction, makes the method more robust, convergence is reached slightly faster and the iterative procedure converges up to $Fr = 0{\cdot}71$, rather beyond the limit shown by the inviscid scheme. It is worth noticing that the introduction of viscosity effects does not cause any significant change in the values of the wave resistance; in fact, as shown in Figure 4, the wave amplitude is very lightly damped. In the same figure the typical non-linear effect of wave steepness can be observed; moreover, with respect to the linear case, a wavelength reduction appears.

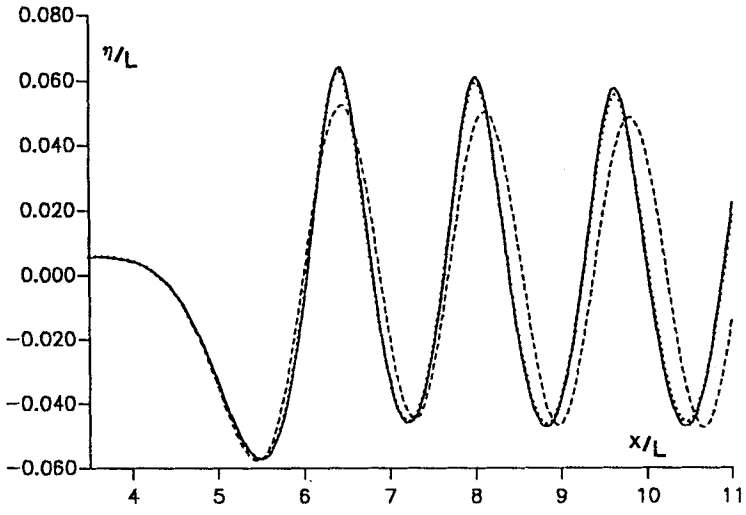

Figure 4. Computed wave profiles: linear (– – –), inviscid non-linear (——) and non-linear with viscous correction (· · · ·). $Fr = 0{\cdot}590\,92$, $h/L = 1{\cdot}376\,15$

The numerical wave profiles obtained by means of the method including viscous effects, for different depths and Froude numbers, are compared in Figure 5 with the experimental data taken from Reference 18 and with the linear solution given by implementing (12′)–(14′). The agreement with the measurements is quite good and the improvement with respect to the linear solution is significant. The importance of non-linear effects in the wave resistance problem is also clearly observed in Figure 6. Anyway, as pointed out in Reference 18, wave resistance measurements for 2D bodies are not so easy to perform and the comparison between the wave profiles is more reliable.

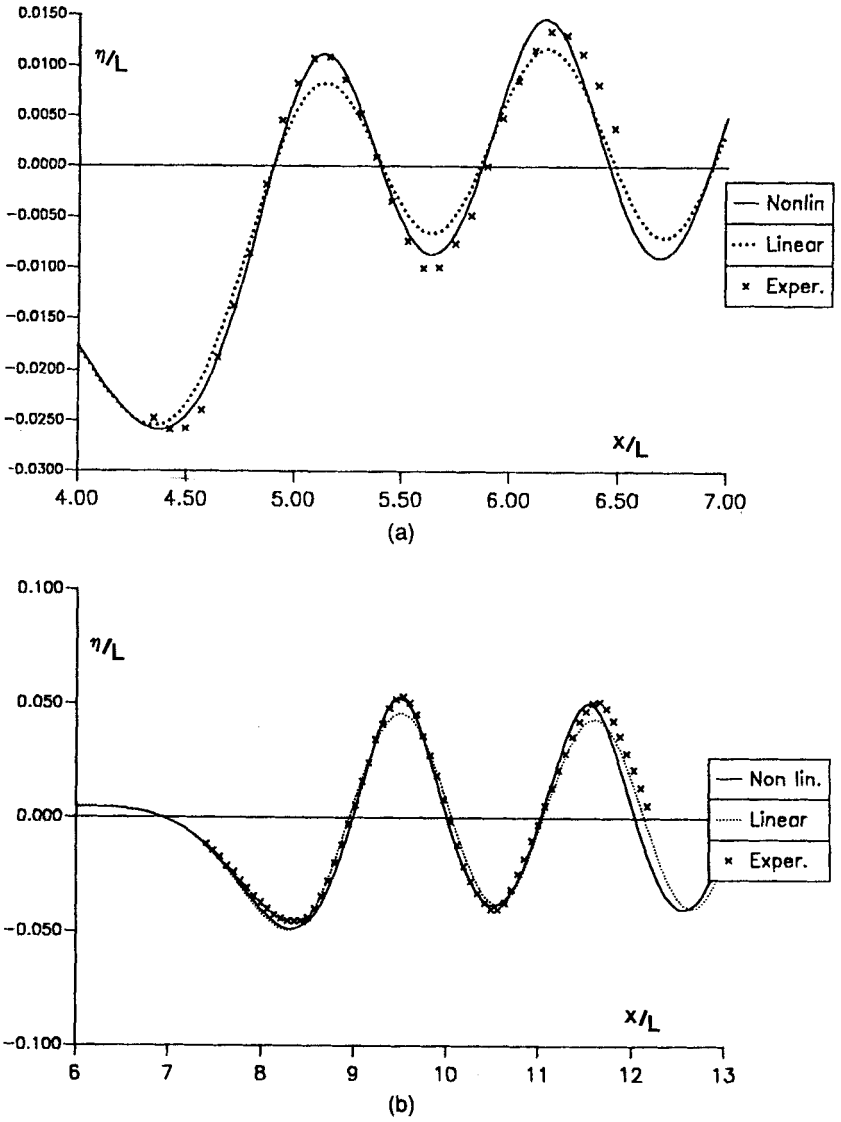

Figure 5. Comparison between the experimental free surface profiles[18] (×) and the numerical solutions: linear (····) and non-linear with viscous correction (——). (a) $Fr=0{\cdot}42208$, $h/L=1{\cdot}14678$. (b) $Fr=0{\cdot}59092$, $h/L=1{\cdot}37615$. (c) $Fr=0{\cdot}59092$, $h/L=1{\cdot}14678$.

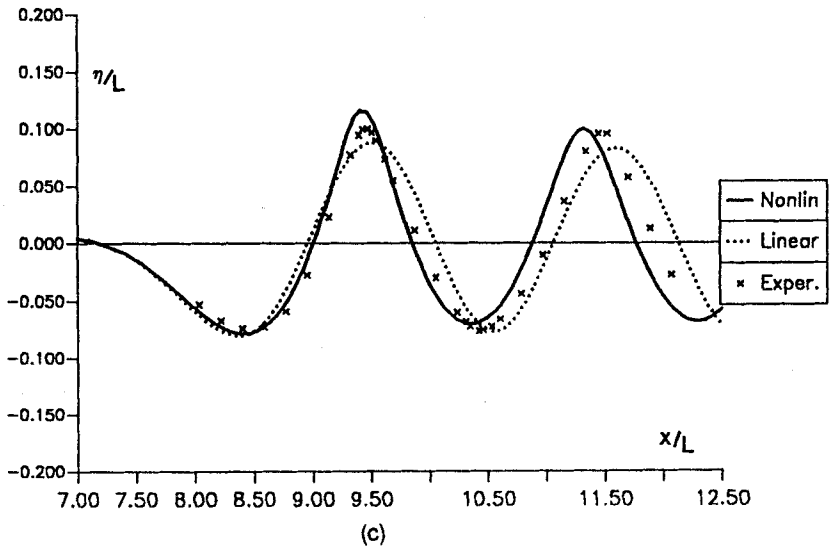

Figure 5. (Continued)

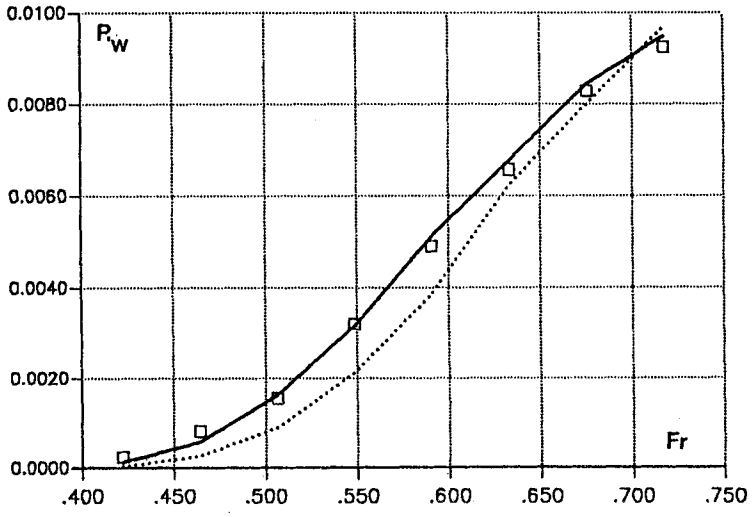

Figure 6. Experimental (□) and numerical wave resistance: linear (···) and non-linear (——)

6. CONCLUDING REMARKS

In the present paper a numerical method to implement the exact free surface steady potential flow formulation has been described. The proposed algorithm, tested with experimental results, seems to be rather reliable. Moreover, both the comparisons with the experimental free surface profiles and wave resistance confirm the importance of the non-linear effects.

Although the computer code has been vectorized, when the number of panels used becomes very large (i.e. more than 1000) and Fr is high (i.e. a smaller relaxation parameter must be used), the iterative procedure quickly becomes very time-consuming. In dealing with the extension to the 3D case, one could consider the use of a quasi-Newton algorithm (e.g. Broyden's method) in the solution of the non-linear system (3′), (11′). Finally, as mentioned before, another natural improvement of this method is the use of the analytical calculation of the derivative $\delta/\delta l$ in (11′).

ACKNOWLEDGEMENTS

This work was supported by the Italian Ministry of Merchant Marine in the frame of the INSEAN research plan 1986.

We would like to acknowledge Professor P. Bassanini (University of Rome) and Professor G. Monegato (University of Turin) for their kind and helpful suggestions and criticisms.

REFERENCES

1. C. Do and P. Guevel, 'Waves on a uniform flow in a channel of constant depth', in A. Fasano and M. Primicerio (eds), *Research Notes in Mathematics, 78, Vol. 1*, pp. 17–28, Pitman, London, 1983.
2. C. W. Dawson, 'A practical computer method for solving ship-wave problems', *2nd Int. Conf. on Numerical Ship Hydrodynamics*, Berkeley, pp. 30–38, University Ext. Publ., CA, 1977.
3. J. L. Hess and A. Smith, 'Calculation of potential flows around arbitrary bodies', *Prog. Aeronaut. Sci.*, Pergamon Press, Vol. 8. (1966).
4. J. V. Wehausen and E. V. Laitone, 'Surface waves', in *Encyclopedia of Physics, Vol. 9*, Springer, Berlin/Gottingen/Heidelberg, 1960.
5. H. C. Raven, 'Variations on a theme by Dawson', *17th Symp. on Naval Hydrodynamics*, The Hague, 1988, pp. 151–171, Nat. Academy Press, Washington D.C., 1989.
6. V. Aanesland, 'A theoretical and numerical study of ship wave resistance', *Ph.D. Thesis*, Department of Marine Technology, The Norwegian Institute of Technology, Trondheim, 1986.
7. P. S. Jensen, 'On the numerical radiation condition in the steady-state ship wave problem', *J. Ship Res.*, **31**(1), 14–22 (1987).
8. P. D. Sclavounos and D. E. Nakos, 'Stability analysis of panel methods for free surface flows with forward speed', *17th Symp. on Naval Hydrodynamics*, The Hague, 1988, pp. 173–193, Nat. Academy Press, Washington D.C., 1989.
9. H. Maruo and S. Ogiwara, 'A method of computation for steady ship waves with nonlinear free surface conditions', *4th Int. Conf. on Numerical Ship Hydrodynamics*, pp. 218–233, Nat. Academy Press, Washington, D.C., 1985.
10. E. F. Campana, F. Lalli and U. Bulgarelli, 'A boundary element method for a nonlinear free surface problem', *Int. j. numer. methods fluids*, **9**, 1195–1206 (1989).
11. A. J. Musker, 'Stability and accuracy of a nonlinear model for the wave resistance problem', *5th Int. Conf. on Numerical Ship Hydrodynamics*, Hiroshima, 1989.
12. G. Jensen, V. Bertram and H. Soding, 'Ship wave-resistance computations', *5th Int. Conf. on Numerical Ship Hydrodynamics*, Hiroshima, 1989, pp. 593–606, Nat. Academy Press, Washington D.C., 1990.
13. O. Daube and A. Dulieu, 'A numerical approach of the nonlinear wave resistance problem', *3rd Int. Conf. on Numerical Ship Hydrodynamics*, Paris, 1981.
14. H. Rong, X. Liang and H. Wang, 'A numerical method for solving nonlinear ship-wave problem', *ITTC*, The Society of Nav. Arch. of Japan, Kobe, 1987.
15. E. F. Campana, F. Lalli, F. Pitolli and U. Bulgarelli, 'Fully nonlinear free surface flow computation by means of moving panels method', *Int. Symp. on Ship Resistance and Powering Performance*, Shanghai, pp. 89–94, 1989.
16. G. K. Batchelor, *An Introduction to Fluid Dynamics*, Cambridge University Press, Cambridge, 1967.
17. T. H. Havelock, 'The wave pattern of a doublet in a stream', *Proc. R. Soc. A* **121**, (1928).
18. N. Salvesen, 'On second order wave theory for submerged two-dimensional bodies', *6th Symp. on Naval Hydrodynamics*, pp. 595–636, Office of Naval Research, Dept. of the Navy, Washington, D.C., 1966.